Table 3. Virology and Microbiology Data*

Case No.	Autopsy Tissue Tested PCR Positive for Coronavirus†	Culture for Coronavirus	IFA Serology for Coronavirus	IF and Isolation for Respiratory Viruses‡	Microbiology Results
			SARS Cases		
1	Lung§	Negative	IgM, IgG seroconversion, 12-d interval	Negative	*Pseudomonas aeruginosa*
2	ETT aspirate, lung§	Negative	IgM, IgG seroconversion, 11-d interval	Negative	Methicillin-resistant *Staphylococcus aureus*
3	Lung	Negative	IgM seroconversion, 8-d interval	Negative	No growth
4	Tracheal swab, spleen, brain, heart, lymph node, lung, and liver	Positive in all except liver	Not done	Negative	No growth
5	Intestine, lymph node, spleen, lung	Positive only in lung	Negative, 6 d apart	Negative	No growth
6	Tracheal swab, heart, lung	Negative	Not done	Negative	No record
7	Heart and lung	Positive	Not done	Negative	α-Hemolytic *Streptococcus* sp, *Klebsiella* sp
8	Heart and lung	Positive	Not done	Negative	No record
			Non-SARS Cases		
9	Negative	Negative	Not done	Culture positive for adenovirus (ETT aspirate, conjunctival swab, intestine, and lung)	No growth
10	Negative	Negative	Not done	Negative	*Pseudomonas aeruginosa, Candida tropicalis, Candida glabrata*
11	Negative	Negative	Not done	Negative	*Streptococcus pneumoniae*
12	Negative	Negative	Negative, 6 d apart	Negative	*Acinetobacter baumanii, Enterococcus* sp, methicillan-resistant *Staphylococcus aureus*
13	Negative	Negative	Not done	Negative	*S pneumoniae, Enterobacter* sp
14	Negative	Negative	Not done	Negative	No record

* SARS indicates severe acute respiratory syndrome; PCR, polymerase chain reaction; IFA, immunofluorescent assay; IF, immunofluorescence; IgM and IgG, immunoglobulins M and G; and ETT, endotracheal tube.
† Autopsy tissue taken for virology testing includes ETT swabs/aspirates, lung, lymph node, spleen, brain, heart, liver, and intestine.
‡ IF testing for respiratory viruses includes respiratory syncytial virus; parainfluenza 1, 2, and 3; influenza A and B; and adenovirus.
§ PCR testing by Defense Medical Research Laboratory.

Table 4. In Situ Hybridization (ISH) Results in Severe Acute Respiratory Syndrome (SARS) Cases*

Case No.	DAD Acute	DAD Organizing	Bronchus
1	Negative	Negative	Negative
2	Negative	Negative	Negative
3	Negative	Negative	NA
4	Positive	Positive	Negative
5	Negative	Negative	Negative
6	Negative	Negative	Negative
7	Positive	NA	NA
8	Positive	NA	NA

* ISH-AT tailing–catalyzed signal amplification of lung from the 8 SARS cases using antisense probe to the nucleocapsid protein of the SARS coronavirus. DAD indicates diffuse alveolar damage; NA, not available for testing.

The clinical course for the 8 SARS patients of our study varied (see Figures 1 through 5). Patients 1, 2, and 3 stayed a mean average of 10 days (range, 10–13) in the hospital, received mechanical ventilation for 7 days (range, 4–8), and died about 3 weeks into their illness. Patients 4 and 5 died within 5 to 8 days of the detection of fever. Patient 4 had significant comorbid factors such as end-stage renal failure and ischemic heart disease. His last admission was for an elevated temperature of 38.5°C. Patient 5 had hypertension and was admitted with a temperature of 35°C and a blood pressure level of 80/50 mm Hg. Patient 6 was febrile, deteriorated rapidly for 2 days, and collapsed 10 days after the onset of fever. Patient 8 saw his general practitioner twice for 1 week for fever (37.7°C) but collapsed at home on day 8. The most rapid onset documented was in case 7, in which the patient had visited a physician 2 days before she died with complaints of fever and a runny nose. Her temperature was recorded on the 2 days preceding her death as 38°C and, without the use of antipyretics, as 37.4°C.

Virology

Virology data are summarized in Table 3. Tissue from the lung yielded positive polymerase chain reaction results in all 8 patients, while heart tissue was positive in 4 of 8 patients. The SARS coronavirus was successfully iso-

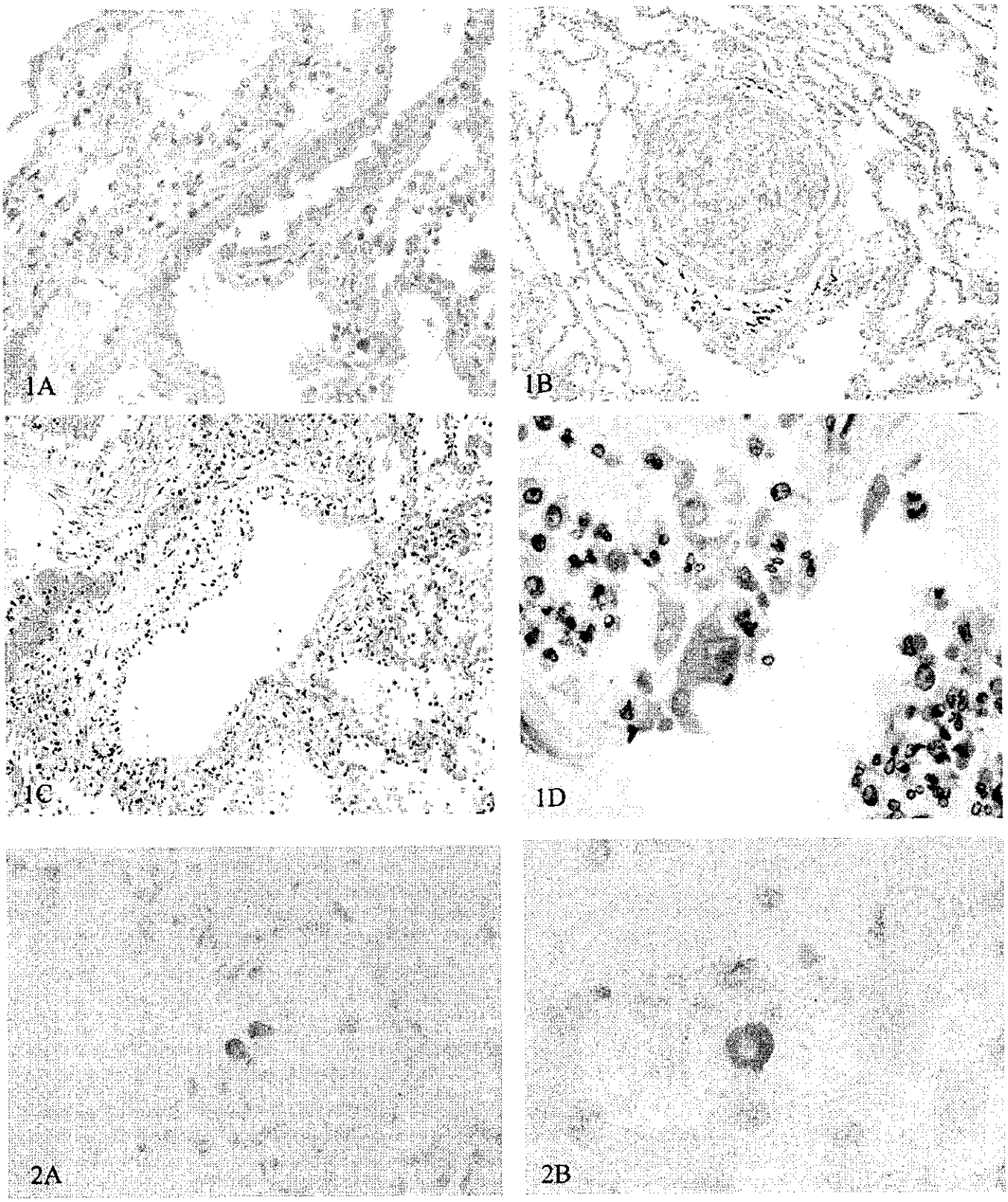

Figure 1. *Diffuse alveolar damage in severe acute respiratory syndrome. A, Acute-phase diffuse alveolar damage from case 7 (hematoxylin-eosin, original magnification ×400). B, Fibrin thrombi in acute-phase diffuse alveolar damage, case 8 (hematoxylin-eosin, original magnification ×200). C, Necrosis of bronchiole mucosa, case 6 (hematoxylin-eosin, original magnification ×200). D, Atypical epithelial cell, case 3 (hematoxylin-eosin, original magnification ×1000).*

Figure 2. *A and B, In situ hybridization for severe acute respiratory syndrome coronavirus, case 7. Positive signal located in the cytoplasm of cells lining the alveolar walls (antisense NP probe, AT tailing amplification, diaminobenzidine chromagen with hematoxylin counterstain, original magnifications ×400 [A] and ×1000 [B]).*

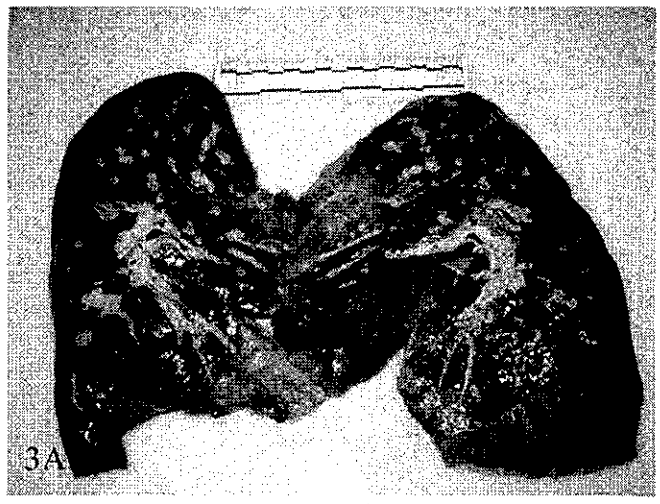

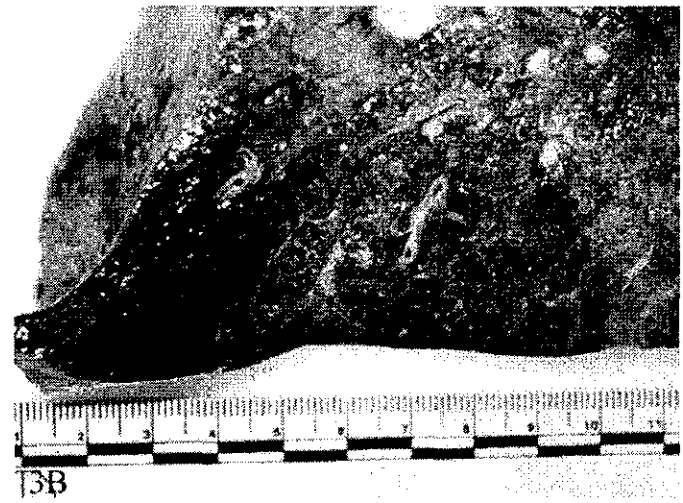

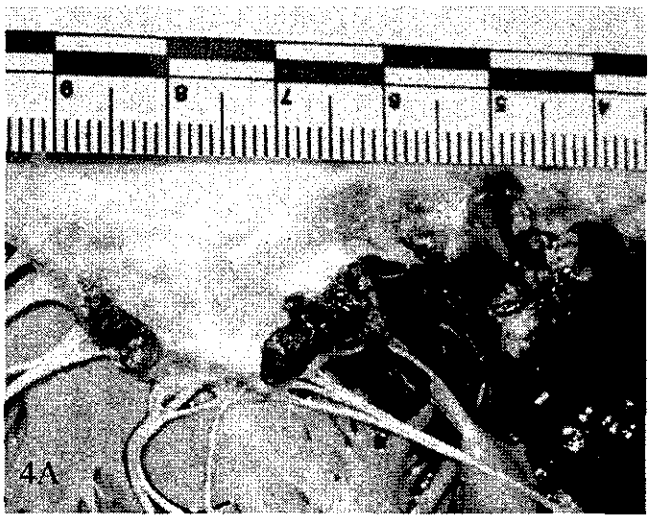

Figure 3. *Gross appearance of lung with diffuse alveolar damage from severe acute respiratory syndrome (SARS) and non-SARS cases at autopsy. A, SARS lung from case 4 showing reddish, meaty appearance with poor aeration. B, SARS lung from case 2, showing a grayish, solid, meaty appearance with hemorrhagic infarct. C, Adenovirus pneumonia, case 9, showing small, pale nodules distributed diffusely through the lung parenchyma. D, Streptococcal pneumonia, case 11 with a septic infarct.*

Figure 4. *Multiple pathology in severe acute respiratory syndrome. A, Case 2 had large, friable vegetations along the valve edge. B, Light microscopy confirms the presence of fibrin (hematoxylin-eosin, original magnification ×40).*

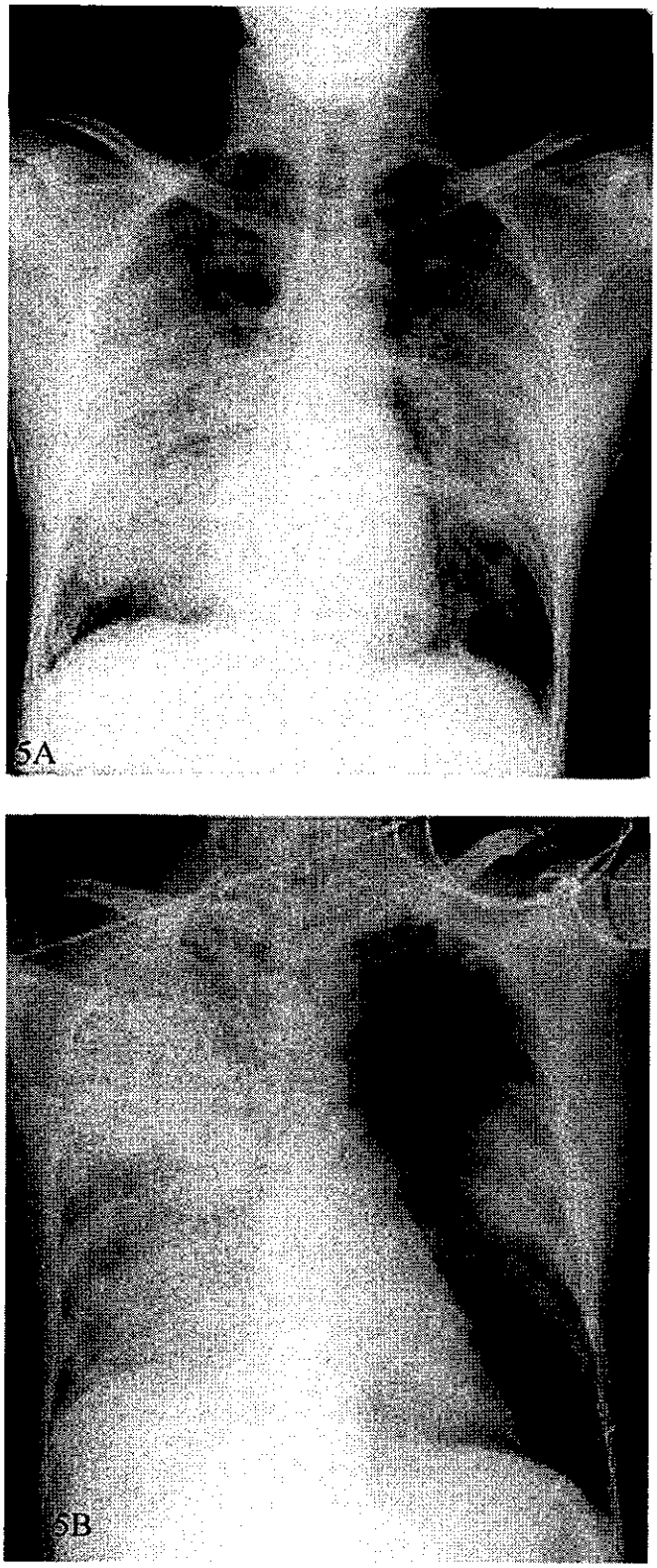

Figure 5. *Chest radiographs in severe acute respiratory syndrome (SARS) and non-SARS. A, Chest radiograph in more advanced stages of a SARS coronavirus infection showing bilateral, diffuse, ground-glass shadowing with consolidation at the periphery of both lungs. B, Chest radiograph from a non-SARS case showing lobar consolidation involving the right upper and lower lobes with air bronchograms. A focus of consolidation is seen at the left middle zone.*

lated from patients 4, 5, 7, and 8, and the adenovirus was isolated from patient 9.

Patients 1, 2, 3, 5, and 12 had an immunofluorescent assay for antibodies to the coronavirus. Of these, patients 1, 2, and 3 showed seroconversion from negative to positive during an 8- to 12-day period. Patients 5 and 12 did not show seroconversion; however, the paired sera available for assay were collected during a shorter 6-day interval, during which seroconversion may not have occurred.

Epidemiology

Nine of 14 patients were known to have had possible exposure to SARS. Patients 1 and 2 were family members or friends of Singapore's first index case/patient. Patient 3 was a separate imported case with a history of travel to Hong Kong. Six patients (4, 5, 6, 10, 12, and 13) were linked to hospitals, while 5 patients (7, 8, 9, 11, and 14) did not have definite links at the time of autopsy.

Radiology

Plain chest x-ray films were available for review at autopsy from 9 of 11 patients. The 3 patients with sudden unexpected death had received no prior radiologic examination.

In the radiographs of 6 of the SARS patients, the early changes were seen as patchy ground-glass opacities, distributed mainly in the central and peripheral areas of the middle and lower zones of the lungs (6 of 6 patients). In 5 patients, these changes were seen in the initial x-ray films. In the non-SARS cohort, the initial x-ray films showed a bilateral reticular interstitial pattern (patient 9), a lobar consolidation in the right lung (patient 11), and a normal chest radiograph (patient 12).

In the SARS cohort, the later radiographs showed bilateral, symmetric, diffuse, ground-glass opacities with patchy consolidation.

Pathology

Pulmonary.—The main pathology in these 14 cases concerned the pulmonary system. All of the patients had heavy lungs that were firm and poorly aerated with minimal edema. Seven of the 14 patients had lung weights greater than 1000 g per lung. The appearance of the patients' lungs at autopsy is described in Table 1.

Thirteen of the 14 patients had diffuse alveolar damage on light microscopy. Of the non-SARS cases, 2 had known risk factors[13–15] for diffuse alveolar damage, such as trauma (patient 13) and surgery with septicemia (patient 12). In 3 patients, classic patterns of infections known to be associated with hyaline membrane formation,[13] such as adenovirus pneumonia (patient 9), *Streptococcus pneumoniae* (patient 11), and fulminant *Pneumocystis carinii* pneumonia (patient 14), were seen.

Patient 10 developed respiratory distress following aortofemoral bypass surgery. The differential diagnosis considered clinically was between a nosocomial infection and SARS, as he had been exposed to the infection during surgery. At autopsy, however, he had asymmetrically heavy lungs (right lung, 1309 g; left lung, 434 g), which suggested lobar pneumonia rather than diffuse alveolar damage or ARDS, in which involvement tends to be diffuse and bilateral. Histologic examination showed a suppurative process with abundant neutrophils and the presence of fungal yeast cells.

The 8 SARS cases (patients 1–8) showed diffuse alveolar

damage[16] with varying degrees of organization. Macrophages were present in the alveolar spaces, and lymphocytes were sparse. Patients 1, 2, and 3 received mechanical ventilation, ribavirin, and corticosteroid therapy. These patients showed acute and organizing phases of diffuse alveolar damage characterized by hyaline membranes and interstitial edema in the former, and interstitial and air space organization in the latter. Atypical pneumocytes, giant cells, and syncytia were noted in the patients who had spent longer periods in the ICU and undergone mechanical ventilation. Although striking, these changes were thought to be within the spectrum of severe diffuse alveolar damage.[13,14]

Patient 5 showed a mixture of acute-phase and organizing-phase diffuse alveolar damage, while patients 4, 6, 7, and 8 showed predominantly the acute phase of diffuse alveolar damage. *Pseudomonas aeroginosa* and methicillin-resistant *Staphylococcus aureus* were identified in 2 of 8 SARS patients, and both of these patients had been treated with corticosteroids. An α-hemolytic *Streptococcus* sp was identified in patient 7, and fungal hyphae suggestive of *Aspergillus* and *Mucor* were observed on light microscopy in patient 5. Neither of these patients received corticosteroid therapy.

In situ hybridization-AT tailing–catalyzed signal amplification staining using the oligonucleotide probe to the nucleocapsid protein region of the SARS coronavirus was positive in 3 of 8 SARS patients. The cytoplasm of occasional cells lining the alveoli and sparse cells within the alveolar lumen gave a positive signal. These were patients 7 and 8, the 2 sudden unexpected deaths, and patient 4, who had a severe and rapidly progressive illness.

Cardiovascular.—Eleven of the 14 autopsies were performed on former hospital inpatients who had spent various amounts of time in the ICU and had received mechanical ventilation. Of the SARS patients, 4 of 8 had pulmonary thromboemboli within the main pulmonary artery or segmental pulmonary arteries identified at autopsy. Three had deep vein thrombosis, which in one patient extended to the paraovarian and parauterine veins. In patient 2, marantic valvular vegetations of approximately 5 to 12 mm in diameter involving the mitral, tricuspid, and aortic valves, along with infarction of the heart, kidneys, and spleen and a 2 × 2-cm softening of the right occipital lobe, were observed. Widespread intravascular fibrin thrombi with infarction of multiple organs were noted in patients 2 and 3.

Heart weights of the patients ranged from 286 to 663 g. Histologic examination of the hearts showed isolated myocardial necrosis in 2 patients, fibrin thrombi within myocardial vessels in 2 patients, and focal perivascular inflammation in 2 patients, but there was no definite histologic evidence of myocarditis. Patient 4 showed significant ischemic cardiac pathology with previous subendocardial infarction and coronary vessel occlusion, suggesting that ischemic cardiac pathology contributed significantly to the cause of death.

Other Organs.—Among the SARS patients, changes in the kidneys and liver reflected the severity of the illness. Acute tubular necrosis was seen in 6 of 8 patients, while one showed end-stage nephrosclerosis, and one showed severe autolytic changes. In the non-SARS cohort, 3 showed hypertensive nephrosclerosis, one of whom also showed diabetic glomerulosclerosis. Two patients, one SARS (patient 2) and one non-SARS (patient 11), showed fibrin thrombi within the kidney, suggesting the presence of disseminated intravascular coagulation.

In the liver, varying degrees of centrilobular necrosis and steatosis and a mild portal inflammatory infiltrate were seen in the SARS patients.

Examination of the lymph nodes and spleen showed lymphoid depletion in the SARS patients. While use of corticosteroids may have been a factor in 3 of the cases, the possibility of an immunosuppressive effect could not be discounted. Hemophagocytosis was seen in 3 cases. Among the non-SARS cohort, white pulp depletion was noted in one patient and erythrophagocytosis in another.

COMMENT

The primary pathologic finding in the SARS autopsy cases of our study was pulmonary diffuse alveolar damage with frequent superimposed bronchopneumonia. Diffuse alveolar damage is a nonspecific histologic reaction[13–15] that can occur for a variety of reasons, including infection, sepsis, uremia, drug toxicity, and collagen vascular disease, as well as in an idiopathic setting in which the term *acute interstitial pneumonia* is appropriate.[17]

During the first few weeks of the SARS outbreak, the diagnosis of SARS infections was made by exclusion.[12] A suspected case was defined by symptoms and epidemiology, while a probable case was defined as a suspected case with radiographic evidence of infiltrates consistent with pneumonia or respiratory distress syndrome or else a suspected case with autopsy findings of respiratory distress syndrome without identifiable cause. Our series of autopsies illustrates the difficulty of rendering a diagnosis of SARS at autopsy, when contact information and clinical history may be lacking, particularly in the setting of a sudden unexpected death.

In the context of emerging infectious diseases, when the clinical syndromes, modes, and probabilities of transmission are yet to be clarified but when immediate quarantine measures[3,5] must be implemented, the implications of a SARS versus a non-SARS diagnosis are great. In our series, this decision was complex, even after a complete autopsy had been performed. Also, all of the patients' lungs receiving gross examination in our series were heavy, with combined weights (except for those of patient 9) of more than 1000 g. For 7 patients, death certification had to be deferred or amended, pending or following the results of histopathology examination or virology tests. In 2 cases, this resulted in a delay of quarantine orders.

Analysis of the progression of disease was an important diagnostic deciding factor. Five of 6 of the SARS patients in our study had patchy ground-glass opacities on admission to the hospital, while for the sixth patient, radiographic abnormalities were documented on the fifth day. In a retrospective analysis of 31 SARS cases seen in the Department of Diagnostic Radiology at the Tan Tock Seng Hospital, 21 of the 31 patients presented with small (involving less than half of one lung zone) ground-glass opacities, while 11 had patchy consolidation, and 2 had both. Ten patients showed a peripheral distribution of ground-glass opacities, 11 showed both peripheral and central opacities, and 6 showed only central changes. Hilar enlargement suggestive of enlarged lymph nodes, interstitial/reticular patterns (patient 9), and dense lobar consolidation (patient 11) were not seen in the initial x-ray films from SARS patients. This is similar to the pattern reported from Hong Kong.[18]

Approximately 21.3% of the patients at the Tan Tock Seng Hospital entered a rapidly progressive pulmonary phase, and of these, 84% met the criteria for acute lung injury or ARDS and required mechanical ventilation. A review of the radiographs of 30 patients in the ICU taken immediately after intubation revealed bilateral symmetric air space shadowing in 80% of them (24 of 30). The shadowing consisted of ground-glass opacities and consolidation. The mortality rate of this group as of May 2, 2003, was 43%.

In this autopsy population, a rising trend in total white blood cell counts and proportion of neutrophils (Table 2) was noted with clinical deterioration to acute lung injury and ARDS.

Histologic examination of the lungs of the 8 SARS patients showed diffuse alveolar damage[16] as the major underlying pathology, ranging from acute, early-phase diffuse alveolar damage with minimal inflammatory infiltrate, as in patient 7, to organizing-phase diffuse alveolar damage with superimposed pneumonia, as in patients 1, 2, and 3. We believe that the cases of our study demonstrate a continuum of changes, with cases 4 through 6 fitting in between these 2 extremes. Patterns of lymphocytic interstitial pneumonia were not seen.

The pattern and morphologic features associated with influenza pneumonia have been described.[19,20] The influenza A virus infection is known to lead to the necrosis of lung epithelial cells[21] and has been demonstrated in bronchial epithelium using in situ hybridization.[22]

While the SARS-associated coronavirus is thought to be new to the human population,[23] the coronavirus infection is known in animals. Reports from investigators working on the porcine reproductive and respiratory syndrome virus have suggested that this virus also has a tropism for macrophages in the lungs and lymphoid tissues[24] and that both infected and uninfected bystander cells undergo apoptosis.[25] A similar mechanism may contribute toward the changes that occur in human infections.

A SARS coronavirus was recently reported in the alveolar epithelial cells and alveolar macrophages of one patient.[26] In our series, 3 patients showed a presence of the virus by in situ hybridization-AT tailing–catalyzed signal amplification. Positive signals for the virus were seen in the 2 sudden unexpected deaths (patients 7 and 8) with acute-phase diffuse alveolar damage as well as in patient 4, whose illness was complicated by diabetes mellitus and end-stage renal failure. The virus was not detected in patients 1, 2, and 3 with the more advanced phases of diffuse alveolar damage and longer periods of illness, nor was it detected in patients 5 and 6. Although this requires further study, it is possible that in SARS coronavirus pneumonia, the initial severity of epithelial injury is related directly to the presence of a virus in the alveolar lining cells and that continuing lung damage is due to poorly controlled immune-mediated processes. In this setting, sudden unexpected death may occur because of a rapid and extensive loss of alveolar cells.

Pulmonary thromboemboli (3 of 3), deep vein thrombosis (2 of 3), intravascular microthrombi (3 of 3), and systemic infarction (1 of 3) were observed in the initial (patients 1–3) autopsies performed. Afterward, surveillance protocols were effected in the Tan Tock Seng Hospital SARS ICU. As of May 2, in the experience of the Tan Tock Seng Hospital SARS ICU, 20.5% had deep vein thrombosis, 11.4%, showed clinical evidence of pulmonary embolism, 15.9% had myocardial infarction, and 4.5% had a cerebrovascular accident. Whether this is related to ARDS and multiorgan pathology in the critically ill,[27–29] therapeutic intervention, or viral-associated damage[21,23] remains to be determined.

The revised World Health Organization definition for SARS,[12] issued on May 1, 2003, was welcome, as it provided for the incorporation of results from laboratory assays for the identification of coronavirus into the definition of SARS cases. We believe that diffuse alveolar damage represents the underlying lung pathology in SARS infections, and we recommend that the Centers for Disease Control and Prevention[30] and World Health Organization[12] case definitions of SARS be modified to specifically mention "pathologic findings of diffuse alveolar damage" rather than "pneumonia or respiratory distress syndrome" of unknown cause, as currently stated.

CONCLUSIONS

In our series of 14 probable and suspected SARS autopsies, 8 could be confirmed as SARS on the basis of virology data. Diffuse alveolar damage was seen as the basic pathology underlying these cases. It is unfortunate that a term such as *atypical pneumonia* has been used in conjunction with SARS. Although nonspecific and generally taken to denote a nonbacterial lung infection,[31] this term does not reflect the underlying dangers of a viral infection with diffuse alveolar damage, which may progress rapidly to ARDS—an entity well known to clinicians.

The patients of our study also showed a wider range of disease manifestation than has been previously described, with 2 presenting at autopsy as sudden unexpected deaths. This is a worrisome finding that illustrates the difficulty of differentiating an important emerging disease from other causes of sudden cardiovascular death at autopsy.

We acknowledge the Defense Medical Research Institute, Singapore, for the polymerase chain reaction results from lung tissue for cases 1 and 2.

References

1. Ksiazek TG, Erdman D, Goldsmith C, et al. A novel coronavirus associated with severe acute respiratory syndrome. *N Engl J Med.* 2003;348:1953–1966.
2. Drosten C, Gunther S, Presier W, et al. Identification of a novel coronavirus in patients with severe acute respiratory syndrome. *N Engl J Med.* 2003;348:1967–1976.
3. Leo YS, Chen M, Heng BH, et al. Centers for Disease Control and Prevention. Severe acute respiratory syndrome—Singapore 2003. *MMWR.* 2003;52:405–411.
4. Poutanem SM, Loe DE, Henry B, et al. Identification of severe acute respiratory syndrome in Canada. *N Engl J Med.* 2003;348:1995–2005.
5. Lipsitch M, Cohen T, Cooper B, et al. Transmission dynamics and control of severe acute respiratory syndrome. Available at: www/scienceexpress.org/23 May 2003/. Accessed May 28, 2003.
6. World Health Organization. Cumulative number of reported probable cases of severe acute respiratory syndrome (SARS), World Health Organization, Communicable Disease Surveillance & Response, update 5 May 2003. Available at: http://www.who.int/csr/sars/country/2003_05_05/en/. Accessed May 7, 2003.
7. Ministry of Health. Annual Statistics Bulletin 2002. Singapore: Health Information Management Branch, Ministry of Health; March 2003:27.
8. Bernard GR, Artigas A, Brigham KL, et al. The American-European Consensus Conference on ARDS: definitions, mechanisms, relevant outcomes and clinical trial coordination. *Am J Respir Crit Care Med.* 1994;149:818–824.
9. The Infectious Diseases Act. Part III Section 9. Cap 137, 1999, rev ed. Available at: http://statutes.agc.gov.sg. Accessed May 17,2003.
10. World Health Organization. PCR primers for SARS by WHO network laboratories. Available at: http://www.who.int/csr/sars/primers/en/. Accessed May 7, 2003.
11. Nakajima N, Ionescu P, Sato Y, et al. In situ hybridization AT-tailing with catalyzed signal amplification for sensitive and specific in situ detection of human immunodeficiency virus-1 mRNA in formalin-fixed and paraffin embedded tissues. *Am J Pathol.* 2003;162:381–389.
12. World Health Organization. Case definitions for surveillance of severe

acute respiratory syndrome (SARS). Revised 1 May 2003. Available at: http://www.who.int/csr/sars/casedefinition/en/. Accessed May 7, 2003.

13. Travis WD, Colby TV, Koss MN, Rosado-de-Christenson ML, Muller NL, King TE. *Nonneoplastic Disorders of the Lower Respiratory Tract.* Washington, DC: Armed Forces Institute of Pathology; 2001. *Atlas of Nontumour Pathology;* 1st series, fascicle 2.

14. Nash G, Blennerhasset JB, Pontoppidan H. Pulmonary lesions associated with oxygen therapy and artificial ventilation. *N Engl J Med.* 1967;276:368–374.

15. Blennerhesset JB. Shock lung and diffuse alveolar damage. Pathological and pathogenetic considerations. *Pathology.* 1985;17:239–247.

16. Franks TJ, Chong PY, Chui P, et al. Lung pathology of severe acute respiratory syndrome: a study of eight autopsy cases from Singapore. *Hum Pathol.* 2003;348:743–748.

17. Travis WD, King TE, Bateman ED, et al. *ATS/ERS International Multidisciplinary Consensus Classification of idiopathic interstitial pneumonia. Am J Respir Crit Care Med.* 2002;165:277–304.

18. Lee N, Hui D, Wu A, et al. A major outbreak of severe acute respiratory syndrome in Hong Kong. *N Engl J Med.* 2003;348:1986–1994.

19. Hers JFAPh, Masurel N, Mulder J. Bacteriology and histopathology of the respiratory tract and lungs in fatal Asian influenza. *Lancet.* 1958;2:1141–1143.

20. Yeldandi AV, Colby TV. Pathologic features of lung biopsy specimens from influenza pneumonia cases. *Hum Pathol.* 1994;25:47–53.

21. Arndt U, Wennemouth G, Barth P, et al. Release of macrophage migration inhibitory factor and CXCL8/interleukin-8 from lung epithelial cells rendered necrotic by influenza A virus infection. *J Virol. 2002;76:9298–9306.*

22. Guarner J, Shieh WJ, Dawson J, et al. Immunohistochemical and in situ hybridization studies of influenza A virus infection in human lungs. *Am J Clin Pathol.* 2000;114:227–233.

23. Holmes KV. SARS-associated coronavirus. *N Engl J Med.* 2003;20:348:1948–1951.

24. Duan X, Nauwynck HJ, Pensaert MB. Virus quantification and identification of cellular targets in the lungs and lymphoid tissues of pigs at different time intervals after inoculation with porcine reproductive and respiratory syndrome virus. *Vet Microbiol.* 1997;56:9–19.

25. Labarque GG, Nauwynck HJ, Van Reeth K, Pensaert MB. Apoptosis in the lungs of pigs during an infection with a European strain of porcine reproductive and respiratory syndrome virus. In: Lavi E, Weiss SR, Hingley ST, eds. *Advances in Experimental Medicine and Biology. The Nidoviruses.* New York, NY: Kluwer Academic/Plenum Publishers; 2001.

26. Nakajima N, Asahi-Ozaki Y, Nagata N, et al. SARS coronavirus-infected cells in lung detected by new in situ hybridization technique. *Jpn J Infect Dis. 2003;56:139–141.*

27. Montgomery AB, Stager MA, Carrico JC, Hudson LD. Causes of mortality in patients with the adult respiratory distress syndrome. *Am Rev Respir Dis.* 1985; 132:485–489.

28. Abraham E. Coagulation abnormalities in acute lung injury and sepsis. *Am J Respir Cell Mol Biol.* 2000;22:401–404.

29. Kolleff MH, Schuster DP. The acute respiratory distress syndrome. *N Engl J Med.* 1995;332:27–37.

30. Centers for Disease Control. Updated interim US case definition of severe acute respiratory syndrome (SARS). May 23, 2003. Available at: http://www.cdc.gov/ncidod/sars/casedefinition.htm. Accessed May 24, 2003.

31. Swartz MN. Approach to the patient with pulmonary infections. *In: Fishman AP, Elias JA, Fishman JA, Grippi MA, Kaiser LR, Senior RM, eds. Fishman's Pulmonary Diseases and Disorders.* 3rd ed. New York, NY: McGraw Hill; 1998.

Journal of Medical Virology 75:295–299 (2005)

Recombinant Nucleoprotein-Based Serological Diagnosis of Crimean–Congo Hemorrhagic Fever Virus Infections

Masayuki Saijo,[1]* Qing Tang,[2] Bawudong Shimayi,[3] Lei Han,[2] Yuzhen Zhang,[4] Muer Asiguma,[4] Dong Tianshu,[4] Akihiko Maeda,[1] Ichiro Kurane,[1] and Shigeru Morikawa[1]

[1]*Department of Virology 1, Special Pathogens Laboratory, National Institute of Infectious Diseases, Musashimurayama, Tokyo, Japan*

[2]*Second Division of Viral Hemorrhagic Fever, Institute of Infectious Diseases Control and Prevention, Chinese Center for Disease Control and Prevention, Beijing, China*

[3]*Bachu County Center for Disease Prevention and Control, Kashi District, Xinjiang Autonomous Region, China*

[4]*Xinjiang Bachu County People's Hospital, Bachu county, Kashi District, the Xinjiang Uygur Autonomous Region, China*

An enzyme-linked immunosorbent assay (ELISA) using recombinant nucleoprotein (rNP) was reported for the detection of immunoglobulin G (IgG) antibodies to Crimean–Congo hemorrhagic fever (CCHF) virus (CCHFV). The immunoglobulin M (IgM)-capture ELISA was developed for the diagnosis of CCHFV infections, using CCHFV rNP as an antigen. These newly developed assays were applied to a study of a CCHF-outbreak and evaluated with sera collected from patients diagnosed as having CCHF by positive reverse transcription-polymerase chain reaction (RT-PCR) and by detection of IgG response. IgM antibodies to CCHFV were detected in 10 of the 13 patients. IgM antibodies to the rNP of CCHFV were detected by the CCHFV rNP-based IgM-capture ELISA in all 6 patients in whom IgG responses were demonstrated, while it was not detected in the 10 patients in whom IgG responses were not demonstrated. Furthermore, the IgM antibodies were detected in 6 of the 61 residents living a CCHF endemic area during the endemic season, while it was not detected in any of the 48 Japanese residents that had never visited the CCHF endemic area. It is concluded that this newly developed CCHFV rNP-based IgM-capture ELISA is a useful method for the diagnosis of CCHFV infections. ***J. Med. Virol. 75: 295–299, 2005.*** © 2004 Wiley-Liss, Inc.

KEY WORDS: Crimean–Congo hemorrhagic fever; CCHF; recombinant nucleoprotein; ELISA; RT-PCR; serological diagnosis

INTRODUCTION

Crimean–Congo hemorrhagic fever (CCHF) virus (CCHFV) is a member of the family Bunyaviridae, genus *Nairovirus* [Nichol, 2001]. CCHF is an acute viral hemorrhagic fever with a high mortality rate of up to 30% [Nichol, 2001]. Humans are infected with the virus by a tick (genus *Hyalomma*) bite or by close contact with freshly slaughtered meat or blood from viremic animals including sheep, cattle, and goats [Nichol, 2001]. CCHFV infections in humans have been reported in Africa, Eastern Europe, the Middle East, and Central and Southern Asia [Hoogstraal, 1979]. The actual number of patients with CCHF is believed to be far greater than that reported, because the disease usually occurs in remote areas. Noscomial outbreaks of CCHF are not rare [Burney et al., 1980; Suleiman et al., 1980; van Eeden et al., 1985; Fisher-Hoch et al., 1995; Papa et al., 2002].

Although there have been no reports of the efficacy of ribavirin therapy for CCHF as evaluated by a control-based study, ribavirin is known to inhibit the replication of CCHFV in vitro and in vivo [Huggins, 1989; Watts et al., 1989; Tignor and Hanham, 1993]. Furthermore, there have been several reports of patients with CCHF treated successfully with ribavirin [van de Wal et al., 1985; Fisher-Hoch et al., 1992; Papa et al., 2002; Tang et al., 2003]. Therefore, the rapid diagnosis of CCHF is important.

The study was performed under the approval of the ethical committee on medical research and human rights, National Institute of Infectious Diseases, Tokyo, Japan.

Grant sponsor: Ministry of Health, Labor, and Welfare of Japan (grant-in-aid).

*Correspondence to: Masayuki Saijo, Department of Virology 1, Special Pathogens Laboratory, National Institute of Infectious Diseases, 4-7-1 Gakuen, Musashimurayama, Tokyo 208-0011, Japan. E-mail: msaijo@nih.go.jp

Accepted 14 October 2004

DOI 10.1002/jmv.20270

Published online in Wiley InterScience (www.interscience.wiley.com)

The CCHFV recombinant nucleoprotein (rNP)-based enzyme-linked immunosorbent assay (ELISA) and immunofluorescent assay are effective for the detection of immunoglobulin G (IgG) antibodies to CCHFV [Saijo et al., 2002a; Saijo et al., 2002b]. Paired serum samples are required for diagnosis by IgG ELISA, because a significant rise in antibody titers must be demonstrated. Detection of immunoglobulin M (IgM) antibodies is another reliable procedure for the rapid diagnosis of CCHF. A patient who was diagnosed as having CCHF by detection of IgM and IgG antibodies using CCHFV rNP-based ELISAs was reported previously [Tang et al., 2003].

In the present study, a CCHFV rNP-based IgM-capture ELISA was evaluated for its efficacy in diagnosis of CCHF using sera collected from patients with acute CCHF confirmed by viral genome amplification with RT-PCR and/or by the detection of IgG responses with rNP-based IgG ELISA. The relationship of IgM and IgG responses determined by the CCHFV rNP-based ELISAs with viremia determined by RT-PCR was examined.

MATERIALS AND METHODS

Serum Samples

The western part of the Xinjiang Uygur Autonomous Region, China, is known to be the site of CCHF outbreaks [Yen et al., 1985; Saijo et al., 2002a; Saijo et al., 2002b; Qing et al., 2003; Tang et al., 2003]. Serum samples drawn from nine patients ("Panel A"), from whom the CCHFV genome was amplified by RT-PCR, in the region during the outbreak seasons in 2001 and 2002 were used. Subsequent serum samples were also collected from five of the nine patients approximately 1 week after the first samples were collected. The time of collection after onset was defined by taking the day on which fever first appeared as day 1. Although the exact days of blood sampling from the other four patients, from whom only the 1st blood samples were drawn, were unclear, these samples were collected within 10 days of onset; i.e., during the acute phase of CCHF. The samples from the two sampling times were designated as 1st and 2nd samples, respectively.

Apart from the nine patients, paired serum samples were collected from 14 individuals ("Panel B") in the same regions in the outbreak season. They were suspected as having CCHF or other viral infections based on clinical manifestations such as fever and joint pain.

There was a relatively large outbreak of CCHF in a small village in the area (data not shown). Serum samples were collected from 61 residents, "Panel C", living in the CCHF endemic area in June 2001, at which time the CCHF outbreak had nearly ended. The age of these residents ranged from 6 to 66 and the male to female ratio was 38:23.

Serum samples collected from 48 Japanese subjects, "Panel D", who had never visited the CCHF endemic area, were used as a control.

The sera used in the present study were collected under informed consent. In the case of unconscious patients and children less than 20 years of age, informed consent was obtained from their family members and parents, respectively.

Positive- and negative-control sera for IgG and IgM-capture ELISA were produced in a monkey (*Macaca fascicularis*) by immunization with the purified His-CCHFV rNP using Inject Alum™ (Pierce Biotechnology, Inc., Rockford, IL) [Saijo et al., 2002b] and were tested by each IgG ELISA and IgM-capture ELISA for verification.

CCHFV rNP-Based IgG ELISA and IgM-Capture ELISA

The CCHFV rNP was expressed as a fusion protein with a 6× His-tag on the N-terminus in the recombinant baculovirus system and was designated CCHFV rNP [Saijo et al., 2002b]. The IgG antibodies to CCHFV were detected by IgG ELISA using CCHFV rNP in the same way as described previously [Saijo et al., 2002b]. The CCHFV rNP-base IgM-capture ELISA was performed as previously reported [Tang et al., 2003].

Reverse Transcription-Polymerase Chain Reaction (RT-PCR)

The details of RT-PCR were also described in a previous paper [Tang et al., 2003].

RESULTS

Cut-Off Values of OD_{405} in IgG and IgM-Capture ELISA

Forty-eight serum samples collected from the "Panel D" subjects were tested as a negative control for the IgM-capture ELISA. The OD_{405}s at a dilution of 1:100 were between −0.17 and 0.15, and the average and standard deviation (SD) at that dilution were −0.008 and 0.071, respectively. The cut-off value, calculated as the average +3SD, was 0.205. Positive and negative results by the IgM-capture ELISA were judged on the basis of this cut-off value at a dilution of 1:100. This cut-off value was applied to the other dilution levels, 1:50, 1:200, and 1:400.

The average and SD values of the adjusted optical density (OD_{405}) at a dilution of 1:400 in the IgG ELISA were 0.069 and 0.039, respectively. Therefore, the cut-off value [average + 3× SD of "Panel D" sera] in the IgG ELISA format measured at a dilution of 1:400 was set at 0.186 in the study. This cut-off value was also applied to the other dilution levels, 1:100, 1:1,600, and 1:6,400.

IgM Responses Determined by IgM-Capture ELISA

The IgM antibody status to CCHFV rNP together with the results of RT-PCR and IgG ELISA are shown in Tables I and II. Positive IgM responses were demonstrated in six of the "Panel A" patients: two in the first

TABLE I. RT-PCR and IgG/IgM Responses to CCHFV rNP in the Serum Samples Drawn From Nine "Panel A" Patients With CCHF as Diagnosed by Positive RT-PCR

	Day(s) after onset, RT-PCR, IgM, and IgG ELISA							
	1st samples (collected within day 3)				2nd samples (collected between days 5 and 11)			
Patient ID	Day(s)[a]	RT-PCR[b]	IgM (OD_{405})[c]	IgG (OD_{405})[d]	Day(s)[a]	RT-PCR[b]	IgM (OD_{405})[c]	IgG (OD_{405})[d]
1	2	+	−(0.035)	−(0.071)	8	+	−(0.065)	−(0.059)
2	2	+	−(0.015)	−(0.071)	10	+	+(0.216)	−(0.058)
3	2	+	−(0.021)	−(0.059)	8	−	+(1.433)	−(0.160)
4[e]	1	+	−(0.020)	−(0.031)	5	−	+(2.711)	+(0.972)
5	3	+	−(0.000)	−(0.007)	11	−	+(1.227)	+(0.235)
6	UK[f]	+	−(0.060)	−(0.181)		ND[g]		
7	UK	+	−(0.016)	−(0.024)		ND		
8	UK	+	+(2.208)	−(0.023)		ND		
9	UK	+	+(0.860)	−(0.019)		ND		

[a]Day(s) after onset was defined by taking the day on which fever first appeared as day 1.
[b]"+" and "−" indicate positive and negative reactions in RT-PCR, respectively.
[c]"+" and "−" indicate positive and negative reactions in IgM-capture ELISA, respectively. The OD_{405} values at a dilution level of 1:100 are shown.
[d]"+" and "−" indicate positive and negative reactions in IgG ELISA, respectively. The OD_{405} values at a dilution level of 1:400 are shown.
[e]This case was reported in the previous report [Tang et al., 2003].
[f]"UK" indicates unknown.
[g]"ND" indicates not drawn.

set of samples and four in the second set of samples (Table I). Positive IgM responses were demonstrated in four of the five patients (Patients 1–5) from whom 2nd samples were collected, but no IgM responses were demonstrated in any of the five 1st samples from these patients (Table I). The IgM antibody to CCHFV was not detected in Patient 1 within 8 days from onset.

Of the nine patients, in whom the CCHFV genome was amplified, a significant rise in IgG antibody titer was demonstrated in two patients (Patients 4 and 5, Table I). Furthermore, a significant rise in IgG antibody titer was demonstrated in 4 individuals (Patients 10–13, Table II) of the 14 "Panel B" patients from whom a paired serum sample was collected. In summary, IgG responses defined as a positive significant rise in IgG antibody titer were demonstrated in six patients. The CCHFV rNP-based IgM-capture ELISA showed a positive reaction in the sera collected from all of the 6 patients (Table II), while it did not show a positive reaction in the sera collected from the other 10 "Panel B" patients, in whom IgG responses were not demonstrated.

Relationship of IgM, IgG Responses, and Viremia

The 1st and 2nd blood samples were drawn from five of the "Panel A" patients. The relationship between the time of sample collection after onset and antibody responses was evaluated in these patients.

IgM and IgG responses were demonstrated in four (80%) and two (40%) of the 2nd samples collected between day 5 and day 11, respectively, while no antibody responses were demonstrated in the 1st samples collected within 3 days after onset (Table I). On the other hand, all the 1st samples and two of the 2nd samples showed a positive reaction in RT-PCR (Table I).

Antibody Responses and Viremia

The relationship between the IgM responses and viremia was evaluated using the serum samples collected from the "Panel A" patients (Table I). Only 3 of the 11 RT-PCR-positive sera (27%) were positive by the IgM-capture ELISA, while all of the 3 RT-PCR-

TABLE II. IgM Responses to CCHFV rNP in Six Patients With CCHF Diagnosed by Positive IgG Responses Determined by CCHFV rNP-Based IgG ELISA

		OD_{405}s in IgM-capture (1:100), IgG ELISAs (1:100), and antibody titers					
		1st samples (within day 3)		2nd samples (days 8–14)		3rd samples (3–4 weeks from onset)	
Panel	Patient ID	IgM	IgG	IgM	IgG	IgM	IgG
A	4	0.020, <50	0.031, <100	2.711, ≥400	0.972, 1,600	ND[a]	ND
	5	0.000, <50	0.007, <100	1.227, ≥400	0.235, 400	ND	ND
B	10	0.159, <50	0.181, <100	0.359, 200	1.412, >6,400	ND	ND
	11	0.184, <50	0.128, <100	1.077, ≥400	1.408, >6,400	ND	ND
	12	ND	ND	3.129, ≥400	0.119, <100	2.761, ≥400	>3.500, ≥6,400
	13	ND	ND	3.147, ≥400	0.367, 400	2.669, ≥400	1.943, ≥6,400

[a]"ND" indicates not drawn.

negative samples were positive by the IgM-capture ELISA (Table I). In contrast, viral RNA was amplified by RT-PCR in all of the 11 IgM-negative and IgG-negative, in 3 of the 4 IgM-positive and IgG-negative samples, and in neither of the 2 IgM-positive and IgG-positive samples.

IgM and IgG Antibodies to CCHFV Among Residents in CCHF Endemic Area During the Outbreak Season

Of the 61 "Panel C" sera, 5 showed positive reactions by both IgM-capture and IgG ELISAs, 1 showed positive reaction by the IgM-capture ELISA only, 13 showed positive reactions by the IgG ELISA only, and the rest showed negative reactions by both IgM-capture and IgG ELISAs. Clinical manifestations in four of the six IgM-positive patients were available. All four patients had fever, headache, and backache. Two of the four had symptoms of nasal and gingival hemorrhage.

DISCUSSION

Patients with CCHF are usually seen in very remote areas and the number of patients with CCHF is relatively small. Patients with suspected CCHF do not always visit hospitals for treatment in CCHF endemic areas, because of economic difficulties and problems in gaining access to hospitals. Furthermore, the facilities at the hospitals in such remote areas are usually not adequate for virological testing or for storing serum samples. Therefore, virological testing of CCHF, and the collection and storage of blood samples are very difficult. Under such difficult conditions, the serum samples of patients with and without CCHF in one CCHF endemic area in the western part of the Xinjiang Uygur Autonomous Region were collected. The serum samples collected from 132 subjects including 13 CCHF-patients were used in the present study. Therefore, it is considered to be acceptable to draw conclusions regarding the efficacy of the rNP-based ELISA for serological diagnosis of and epidemiological study on CCHF by analyzing the data obtained in this study.

The patients with positive IgG responses, taken as the detection of a significant rise in IgG antibody titer determined by CCHFV rNP-based IgG ELISA, are considered to be CCHF-positive patients, because the IgG ELISA has been confirmed to have high sensitivity and specificity in detecting specific IgG antibodies to CCHFV [Saijo et al., 2002b]. Within this limited number of patients, the efficacy of the CCHFV rNP-based IgM ELISA in diagnosis of CCHF and the relationship between time after onset, antibody responses, and viremia were evaluated.

Six of the nine "Panel A" patients were confirmed to be IgM-positive by CCHFV rNP-based IgM-capture ELISA. The blood samples of the other three "Panel A" patients with IgM-negative result were collected within about 10 days after onset. If the blood had been collected a little later, IgM responses to CCHFV rNP would have been detected. IgM antibodies to CCHFV were detected in all the 6 patients with IgG responses to CCHFV (Table II), while no IgM antibodies were detected in any of the other 10 "Panel B" individuals in whom IgG responses not demonstrated. IgM antibodies to CCHFV were demonstrated in 6 of the 61 serum samples collected from the "Panel C" residents living in a CCHF endemic area during the outbreak season, while none of the Japanese sera showed a positive reaction in the IgM-capture ELISA. These data indicate that the IgM-capture ELISA using His-CCHFV rNP has high sensitivity and specificity in detecting IgM antibodies to CCHFV and that it is useful for the rapid and accurate diagnosis of CCHF. If the sensitivity and specificity are analyzed using the paired sera collected from 14 "Panel B" subjects composed of 4 CCHF-patients and 10 non-CCHF-patients, both the sensitivity and specificity would be considered to be 100%.

Although, further study is needed, the data in the present study suggest that the IgM antibodies to CCHFV become detectable within at least 2 weeks from onset. It was found that viremia was still present at the stage in which positive IgM responses but not IgG responses were observed and that the viremia was already eliminated at the stage in which positive IgG responses were observed. To increase the sensitivity in detecting viremia, nested RT-PCR was performed for serum samples. However, mononuclear phagocytes are one of the main targets of CCHFV infections [Burt et al., 1997]. Therefore, it is possible that the sensitivity of the nested RT-PCR for detection of the CCHFV genome increases when whole blood samples rather than serum samples are used.

The effectiveness of the newly developed CCHFV rNP-based IgM-capture ELISA for the diagnosis of CCHF should be compared with that of the already developed methods such as indirect immunofluorescence assay [Fisher-Hoch et al., 1992; Burt et al., 1998; Papa et al., 2002] and/or IgM-capture ELISA [Saluzzo and Le Guenno, 1987; Gonzalez et al., 1990; Chapman et al., 1991; Burt et al., 1994; Khan et al., 1997; Rodriguez et al., 1997; Schwarz et al., 1997] using authentic CCHFV antigens. However, CCHFV is regarded as a biosafety level-4 (BLS-4) pathogen in Japan, and viral antigen preparation is difficult. Therefore, the CCHFV rNP-based IgM-capture ELISA was not compared with IgM antibody detection systems using authentic viral antigens. The inability to produce authentic viral antigens was overcome by evaluating the CCHFV rNP-based IgM capture ELISA using the sera collected from patients with and without CCHF.

The main antigenic region in the NP of CCHFV (482 amino acid residues) was located on the central portion from amino acid positions 201 to 306 as reported previously [Saijo et al., 2002b]. The amino acid sequence of this region in NP (Chinese strain 8402) has 97%–100% homology to the other Chinese strains and 92%–96% homology to non-Chinese strains. Furthermore, the antibodies to CCHFV in Asian patients with CCHF were detected by the IgG ELISA using the recombinant NP of CCHFV strain IbAr 10200 (GenBank accession no.

U88410, data not shown). These results indicate that the IgM-capture ELISA using the CCHFV rNP of Chinese strain 8402 might be useful in detecting not only antibodies to CCHFV Chinese strains but also antibodies to strains in other regions.

As CCHFV is a BSL-4 pathogen, the preparation of the CCHFV antigen must be performed in a BSL-4 laboratory and this restriction makes the preparation of CCHF antigens difficult in institutes without a BLS-4 laboratory. It was demonstrated that the rNP-based IgM-capture ELISA offers a definite advantage in the diagnosis of and seroepidemiological study on CCHF. In summary, diagnosis by the combination of IgM-capture ELISA and RT-PCR is more sensitive, accurate, and reliable than that by either single method.

ACKNOWLEDGMENTS

We thank all the staff in the Xinjiang Bachu People's Hospital who contributed to the treatment of the patients. We also thank Dr. Li Fan, Director of the AIDS Prevention and Control Center, Xinjiang Epidemic Prevention Station, Urumqi, the Xinjiang Uygur Autonomous Region, and his colleagues. We are grateful to Ms. M. Ogata, Department of Virology 1, Special Pathogens Laboratory, National Institute of Infectious Diseases, Tokyo, Japan, and Ms. X. Zhao and Ms. X. Tao, the Second Division of Viral Hemorrhagic Fever, Institute of Infectious Disease Control and Prevention, Chinese Center for Disease Control and Prevention, for their excellent technical assistance in this work. The blood samples were drawn carefully from the patients in the hospital. The work dealing with the patients' blood samples was performed in a highly contained laboratory according to the regulations of the Institute of Infectious Disease Control and Prevention, Chinese Center for Disease Control and Prevention.

REFERENCES

Burney MI, Ghafoor A, Saleen M, Webb PA, Casals J. 1980. Nosocomial outbreak of viral hemorrhagic fever caused by Crimean hemorrhagic fever-Congo virus in Pakistan, January 1976. Am J Trop Med Hyg 29:941–947.

Burt FJ, Leman PA, Abbott JC, Swanepoel R. 1994. Serodiagnosis of Crimean–Congo haemorrhagic fever. Epidemiol Infect 113:551–562.

Burt FJ, Swanepoel R, Shieh W, Smith JF, Leman PA, Greer PW, Coffield LM, Rollin PE, Ksiazek TG, Peters CJ, Zaki SR. 1997. Immunohistochemical and in situ localization of Crimean–Congo hemorrhagic fever (CCHF) virus in human tissues and implications for CCHF pathogenesis. Arch Pathol Lab Med 121:839–846.

Burt FJ, Leman PA, Smith JF, Swanepoel R. 1998. The use of a reverse transcription-polymerase chain reaction for the detection of viral nucleic acid in the diagnosis of Crimean–Congo haemorrhagic fever. J Virol Methods 70:129–137.

Chapman LE, Wilson LM, Hall DB, LeGuenno B, Dykstra EA, Ba K, Fisher-Hoch SP. 1991. Risk factors for Crimean–Congo hemorrhagic fever in rural northern Senegal. J Infect Dis 164:686–692.

Fisher-Hoch SP, McCormick JB, Swanepoel R, Van Midderlkoop A, Harvey S, Kustner HG. 1992. Risk of human infections with Crimean–Congo hemorrhagic fever virus in a South African rural community. Am J Trop Med Hyg 47:337–345.

Fisher-Hoch SP, Khan JA, Rehman S, Mirza S, Khurshid M, McCormick JB. 1995. Crimean–Congo haemorrhagic fever treated with oral ribavirin. Lancet 346:472–475.

Gonzalez J, LeGuenno B, Guillaud M, Wilson ML. 1990. A fatal case of Crimean–Congo haemorrhagic fever in Mauritania: And serological evidence suggesting epidemic transmission. Trans Royal Trop Med Hyg 84:573–576.

Hoogstraal H. 1979. The epidemiology of tick-borne Crimean–Congo hemorrhagic fever in Asia, Europe, and Africa. J Med Entomol 15: 307–417.

Huggins JW. 1989. Prospects for treatment of viral hemorrhagic fevers with ribavirin, a broad spectrum antiviral drug. Rev Infect Dis ii:S750–S761.

Khan AS, Maupin GO, Rollin PE, Noor AM, Shurie HH, Shalabi AG, Wasef S, Haddad YM, Sadek R, Ijaz K, Peters CJ, Ksiazek TG. 1997. An outbreak of Crimean–Congo hemorrhagic fever in the United Arab Emirates, 1994-1995. Am J Trop Med Hyg 57:519–525.

Nichol ST. 2001. Bunyaviruses. In: Knipe DM, Howley P, editors. Fields virology, 4th ed. Philadelphia, PA: Lippincott-Raven, pp 1603–1633.

Papa A, Ma B, Kouidou S, Tang Q, Hang C, Antoniadis A. 2002. Genetic characterization of the MRNA segment of Crimean–Congo hemorrhagic fever virus strains, China. Emerg Infect Dis 8:50–53.

Qing T, Saijo M, Lei H, Maeda A, Ikegami T, Xinjung W, Kurane I, Morikawa S. 2003. Detection of immunoglobulin G to Crimean–Congo hemorrhagic fever virus in sheep sera by nucleoprotein-based enzyme-linked immunosorbent and immunofluorescence assays. J Virol Methods 108:111–116.

Rodriguez LL, Maupin GO, Ksiazek TG, Rollin PE, Khan AS, Schwarz TF, Lofts RS, Smith JF, Noor AM, Peters CJ, Nichol ST. 1997. Molecular investigation of a multisource outbreak of Crimean–Congo hemorrhagic fever in the United Arab Emirates. Am J Trop Med Hyg 57:512–518.

Saijo M, Qing T, Niikura M, Maeda A, Ikegami T, Sakai K, Prehaud C, Kurane I, Morikawa S. 2002a. Immunofluorescence technique using HeLa cells expressing recombinant nucleoprotein for detection of immunoglobulin G antibodies to Crimean–Congo hemorrhagic fever virus. J Clin Microbiol 40:372–375.

Saijo M, Qing T, Niikura M, Maeda A, Ikegami T, Prehaud C, Kurane I, Morikawa S. 2002b. Recombinant nucleoprotein based enzyme-linked immunosorbent assay for detection of immunoglobulin G to Crimean–Congo hemorrhagic fever virus. J Clin Microbiol 40: 1587–1591.

Saluzzo J, Le Guenno B. 1987. Rapid diagnosis of human Crimean–Congo hemorrhagic fever and detection of the virus in naturally infected ticks. J Clin Mircobiol 25:922–924.

Schwarz TF, Nsanze H, Ameen AM. 1997. Clinical features of Crimean–Congo haemorrhagic fever in the United Arab Emirates. Infection 25:364–367.

Suleiman MN, Muscat-Baron JM, Harries JR, Satti AG, Platt GS, Bowen ET, Simpson DI. 1980. Congo/Crimean haemorrhagic fever in Dubai. An outbreak at the Rashid Hospital. Lancet ii:939–941.

Tang Q, Saijo M, Yuzhen Y, Asiguma M, Tianshu D, Han L, Shimayi B, Maeda A, Kurane I, Morikawa S. 2003. A patient with Crimean–Congo hemorrhagic fever serologically diagnosed by recombinant nucleoprotein-based antibody detection systems. Clin Diagn Lab Immunol 10:489–491.

Tignor GH, Hanham CA. 1993. Ribavirin efficacy in an in vivo model of Crimean–Congo hemorrhagic fever virus (CCHF) infection. Antiviral Res 22:309–325.

van de Wal BW, Joubert JR, van Eeden PJ, King JB. 1985. A nosocomial outbreak of Crimean–Congo haemorrhagic fever at Tygerberg Hospital. Part IV. Preventive and prophylactic measures. S Afr Med J 68:729–732.

van Eeden PJ, Joubert JR, van de Wal BW, King JL, de Kock A, Groenewald JH. 1985. A nosocomial outbreak of viral hemorrhagic fever caused by Crimean–Congo haemorrhagic fever at Tygerberg Hospital. Part I. Clinical features. S Afr Med J 68:711–717.

Watts DM, Ussery MA, Nash D, Peters CJ. 1989. Inhibition of Crimean–Congo hemorrhagic fever viral infectivity yields in vitro by ribavirin. Am J Trop Med Hyg 41:581–585.

Yen YC, Kong LX, Lee L, Zhang YQ, Li F, Cai BJ, Gao SY. 1985. Characteristics of Crimean–Congo hemorrhagic fever virus (Xinjiang strain) in China. Am J Trop Med Hyg 34:1179–1182.

Arch Virol (2004) 149: 1279–1292
DOI 10.1007/s00705-004-0306-y

Archives of Virology
Printed in Austria

Modification of endothelial cell functions by hantaan virus infection: prolonged hyper-permeability induced by TNF-alpha of hantaan virus-infected endothelial cell monolayers

M. Niikura[1], **A. Maeda**[1], **T. Ikegami**[1,2], **M. Saijo**[1], **I. Kurane**[1], and **S. Morikawa**[1]

[1]Department of Virology 1, National Institute of Infectious Diseases, Musashimurayama, Japan
[2]Department of Biomedical Science, Graduate School of Agricultural and Life Sciences, The University of Tokyo, Tokyo, Japan

Received November 26, 2003; accepted January 28, 2004
Published online March 25, 2004

Summary. Serious vascular leakage is central to the pathogenesis of hantavirus infections. However, there is no evidence suggesting the hantavirus infection of endothelial cells directly causes obvious cell damage or morphological alteration either *in vivo* or *in vitro*. In this study, we examined whether Hantaan virus (HTNV) infection modifies the barrier function of endothelial cell monolayers upon the exposure to pro-inflammatory cytokines. Low levels (1 ng/ml) of tumor necrosis factor-alpha initially increased the permeability in both HTNV-infected and uninfected monolayers similarly. Thereafter, however, these monolayers showed significant difference. The HTNV-infected monolayers remained irreversibly hyper-permeable during the experimental period up to 4 days, while the uninfected monolayers completely recovered the barrier function. The prolonged hyper-permeability of HTNV-infected monolayers was not associated with cell death or gap formation in the monolayers, and was independent from their nitric oxide or prostaglandin production. These results are the first evidence that hantavirus infection modifies barrier function of endothelial cell monolayers and suggest that HTNV-infection of endothelial cells may contribute to the increased vascular leakage through the prolonged response to cytokines.

Introduction

Hantaviruses belong to the family *Bunyaviridae* and are transmitted to humans from various species of rodents, which are the natural reservoirs. Hantaviruses

consist of numerous strains and each strain is maintained in different rodent species in a natural environment [31]. It is believed that the geographical isolation of these host species contributes to the regional variation in the virulence of hantaviruses [38]. The severest forms of the hantavirus infections are typified by hemorrhagic fever with renal syndrome (HFRS) mostly caused by isolates of *Hantaan virus* (HTNV) in eastern Asia and hantavirus pulmonary syndrome (HPS) caused by isolates of *Sin Nombre virus* (SNV), Andes virus and related viruses in Americas [6, 37, 38]. The major target organs appear to be different between these two forms of hantavirus infections: kidneys in HFRS and lungs and hearts in HPS. However, same organs are often affected in both diseases and it is considered that one of the fundamental pathological manifestations is vascular leakage [6, 7, 21, 37, 38].

Both HTNV and SNV infect endothelial and monocytic cells *in vitro* and *in vivo*. Neither hantavirus infections of cultured cells causes obvious cytopathic effects, contrary to some other hemorrhagic fever viruses like filoviruses [17, 36, 39, 43, 45]. In filovirus infection, for example, the disruption of endothelial cells *in vivo* directly relates to the massive vascular leakage [11]. An *in vitro* study showed that HTNV infection induced apoptotic endothelial cell death [16]. Nevertheless, histopathological examinations of either hantavirus-infected patients did not show major endothelial cell death [24, 35, 45]. Further, it was reported that SNV infection of endothelial cell monolayers did not alter the permeability or tight junction structures *in vitro* [17, 42]. It is, therefore, possible that both hantavirus infections affect the function of endothelial cells in a limited fashion.

HTNV-infected patients develop cellular and humoral immune responses before or very soon after the onset of clinical symptoms, leading to a hypothesis that the symptoms are partly due to immunopathogenesis [7]. Animal experiments with HTNV supported this hypothesis [18, 30, 34, 44]. Besides the virus-specific immunity, elevated levels of tumor necrosis factor alpha (TNF-alpha) and interleukin-6 (IL-6) in HFRS patients' sera were reported [22]. In an *in vitro* study, the infection of immature dendritic cells with HTNV weakly up-regulated TNF-alpha production [39]. Similarly, the infection of human alveolar macrophages with SNV *in vitro* resulted in a weak induction of TNF-alpha at around 1 ng/ml in the culture supernatant [17]. Endothelial cells carry two known TNF-alpha receptors, TNF-R75 and TNF-R55 [25, 27]. The effects of TNF-alpha on endothelial cells through these TNF-alpha receptors have been widely investigated. TNF-alpha increases vascular permeability [2, 5, 14, 33, 40]. It induces the release of cytokines and chemokines from endothelial cells [27]. It also up-regulates production of inducible enzymes such as cyclooxygenases-2 (Cox-2) and nitric oxide synthases (NOS) [4, 12, 28]. However, the relevance of these specific and non-specific immune responses elicited by hantavirus infections to their pathogenesis is not yet well understood.

Since neither the increase in permeability of endothelial cell monolayers [42] nor TNF-alpha induction in monocytic cells [17, 39] upon the hantavirus infections *in vitro* alone was accountable levels for the clinical manifestations seen in HFRS, we hypothesized that the low level of pro-inflammatory cytokines produced by HTNV-infected monocytic cells might differently affect HTNV-

infected and uninfected endothelial cells, due to possible functional alterations of the HTNV-infected endothelial cells. In order to test this hypothesis, we compared the responses of HTNV-infected and uninfected human umbilical vein endothelial cells (HUVEC) to low concentrations of cytokines.

Materials and methods

Cells and viruses

Pooled primary HUVEC was purchased from Clonetics (San Diego, CA). HUVECs were expanded and maintained in EGM-2 medium supplemented with growth factors and 2% bovine fetal serum (Bullet kit, Clonetics) as recommended by the supplier. The cells were cultured at 37 °C with 5% CO_2 throughout the experiments. HTNV strain 76–118 was provided by Dr. J. Arikawa (Hokkaido University, Japan) and propagated in Vero E6 cells.

Cytokines, antibodies and specific inhibitors

Recombinant human TNF-alpha was purchased from Lifetech (Rockville, MD). The specific activity was $>2 \times 10^7$ units/mg. Recombinant human IL-6 was purchased from Genzyme (Cambridge, MA). Neutralizing polyclonal antibodies specific to TNF-alpha and IL-6, respectively, were purchased from R&D systems (Minneapolis, MN). Neutralization of TNF-alpha prior to stimulation was achieved by mixing 100 ng/ml TNF-alpha and 50 μg/ml antibody and incubation on ice for 1.5 hr. Polyclonal rabbit antiserum to *Seoul virus* (a hantavirus species) strain SR-11 was prepared in our laboratory by inoculation of the live virus to a rabbit [41]. This antiserum was cross-reactive with HTNV. Monoclonal antibody specific to plakoglobin was purchased from Zymed (South San Francisco, CA). Specific inhibitors for NOS and Cox, aminoguanidine and L-NMA, and indomethacine, respectively, were purchased from Sigma (St. Lois, MO). They were used at the concentrations reported effective, respectively [8, 15, 28].

Preparation of HTNV-infected HUVEC

HUVECs were infected with HTNV at the passage level one and further passed twice. At the passage level of three in total, the HTNV-infected cells were frozen as aliquots in liquid nitrogen. Uninfected cells were similarly passed and frozen at the same passage level. The frozen cells were thawed and cultured in tissue culture flasks. These cells were trypsinized, counted and subjected to the experiments. The HTNV-infected and uninfected HUVECs were compared at the same passage levels between four and six. The percentage of HTNV-infected cells at the passage level four was greater than 50%, when determined by an immunofluorescent assay using the antiserum to Seoul virus. The absence of mycoplasma in both HTNV-infected and uninfected HUVECs was confirmed by a PCR-based kit (Mycoplasma Plus PCR Primer Set, Stratagene, La Jolla, CA).

Transmonolayer electrical resistance (TER) of HUVEC monolayers

TER of the HUVEC monolayers was examined by Endome chamber (World Precisions, Saratoga, FL). HUVECs were plated at a density of 1×10^5 cells per well in Transwell-col (0.33 cm^2 growth area, Coaster, Cambridge, MA) with 0.6 and 0.1 ml of the culture medium in the lower and upper chambers, respectively. The growth area was pre-coated with fibronectin according to the method by Bonner and O'Sullivan [3]. On the next day, the culture medium was carefully removed and the cells were re-fed with the same volumes of medium. Two or three days later, designated as time 0, the TER was measured in Endome chamber filled with

0.6 ml of the medium. All the reagents added to the wells were prepared in the medium as 100× concentrations to the final concentrations, and 1 μl was added to 0.1 ml of the medium present in the upper chambers. All the experiments were performed in triplicate and the results were expressed as averages and standard deviations (SD). The measured resistance was converted to net resistance per cm^2 according to the formula:

"Net resistance per cm^2"
= "[Measured resistance (ohm)-21(ohm, resistance without cell monolayer)]/3"

Permeability assay

Permeability of the HUVEC monolayers was examined as described previously [3]. Briefly, 1 g of bovine serum albumin (BSA, Sigma) was stained with 45 mg of trypan blue (Sigma) by mixing in 5 ml of the medium at room temperature (RT) for 2 hr. The binding of trypan blue to BSA was confirmed by precipitating the stained BSA by trichroloacetic acid. After centrifugation, the remaining free trypan blue in the supernatant was less than 0.07% in comparison with the pre-precipitation solution, when determined by the absorbance at 550 nm. The stained BSA was filter sterilized. To measure the leakage through cell monolayers, 10 μl of the stained BSA was added to the upper chamber of each Transwell containing HUVEC monolayer. After 4 hr of incubation, 100 μl of the medium in lower chambers was removed and the absorbance was measured at 550 nm.

Cell viability assay

Cell viability was examined by Cell Counting Kit-8 (CCK-8), which utilizes water-soluble tetrazolium salt (Dojin Chemical, Tokyo, Japan). The HTNV-infected and uninfected HUVECs were plated in 96-well tissue culture plates pre-coated with fibronectin, at a density of 1×10^5 cells per well in 200 μl of the medium. On the next day, the medium was completely replaced and cells were cultured for additional 2 days. Then TNF-alpha was added to the medium at a final concentration of 1 ng/ml. After 72 hr culture, 10 μl of the tetrazolium salt solution supplied in CCK-8 was added to each well and incubated for 1.5 hr. The culture supernatant (100 μl) was transferred to another 96-well plate and the absorbance was measured at 450 nm by a microplate reader with the reference wavelength at 600 nm.

Immunohistochemistry

The HTNV-infected and uninfected HUVECs were cultured on cover slips pre-coated with fibronectin in 48 well tissue culture plates at a density of 3×10^5 cells per well in 400 μl medium. Prior or after the TNF-alpha treatment, the cells were fixed in 4% formaldehyde at RT. The cells were permealized by 2% NP-40 and stained by anti-plakoglobin mouse monoclonal and anti-Seoul virus rabbit polyclonal antibodies. The reacted antibodies were detected by either FITC-labeled anti-mouse IgG (Zymed) or Rhodamine-labeled anti-rabbit IgG (Jackson ImmunoResearch, West Grove, PA), respectively.

Cytokine assays

IL-6, TNF-alpha and IL-1beta were quantitated by Quantikine ELISA kits (R&D Systems). The HTNV-infected and uninfected HUVECs (2.5×10^5 cells) were plated in 1 ml medium in 24 well tissue culture plates pre-coated with fibronectin. The medium was replaced on the

next day and cultured for additional 2 days. Before the addition of 1 ng/ml of TNF-alpha, the first sample was collected (time 0). After the indicated hours of culture, the supernatant (100 μl) was recovered from each well. The supernatants were kept at −80 °C until use.

Statistical analyses

Student's T-tests were performed using Microsoft Excel software.

Results

Effect of TNF-alpha on HTNV-infected endothelial cell monolayers

The transmonolayer electrical resistance (TER) of HUVEC monolayers was not changed by HTNV infection alone (Fig. 1A, time 0). The TER of HTNV-infected and uninfected monolayers was between 10 and 20 ohm/cm^2, which was comparable to the previous reports [2]. TNF-alpha significantly decreased the TER of HTNV-infected and uninfected monolayers at 1 ng/ml (Fig. 1A) and 10 ng/ml, but not at 0.1 ng/ml (data not sown). The HTNV-infected and uninfected monolayers showed similar levels of TER decrease as early as 4 hr after the addition of 1 ng/ml of TNF-alpha (Fig. 1A). The duration of the effect was, however, significantly different between the HTNV-infected and uninfected monolayers. In the uninfected monolayers, the decreased TER started to recover after 24 hr

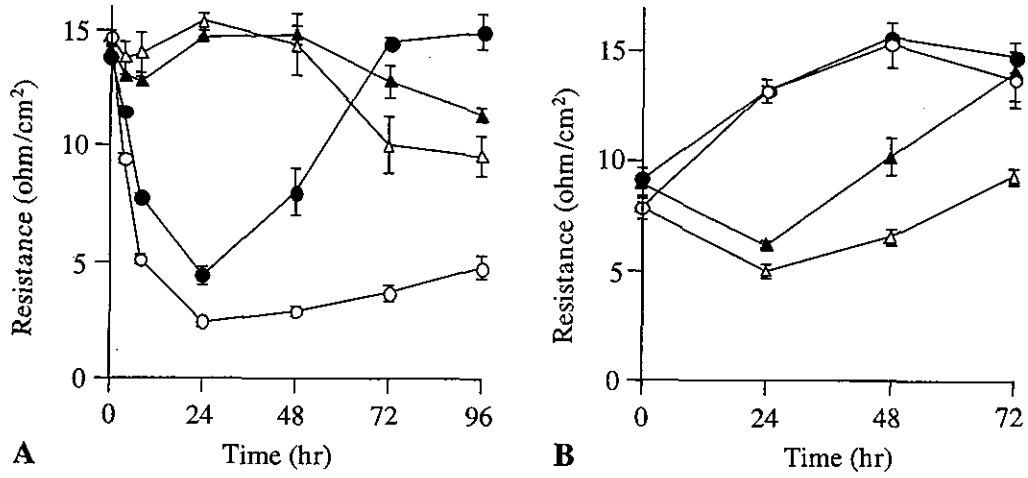

Fig. 1. Effect of TNF-alpha at 1 ng/ml on transmonolayer electrical resistance (TER) of HTNV-infected and uninfected HUVEC. **A.** HTNV-infected (○) and uninfected (●) monolayers were stimulated by TNF-alpha at time 0 and the TER was measured at 4, 8, 24, 48, 72 and 96 hr after stimulation. Unstimulated controls of HTNV-infected (△) or uninfected (▲) HUVEC monolayers were included. **B.** Contribution of TNF-alpha to the decreased TER after TNF-alpha stimulation. TNF-alpha was mixed with neutralizing antibody specific to TNF-alpha. After 1.5 hr incubation on ice, the neutralized (○, infected; ●, uninfected) or mock-neutralized (△, infected; ▲, uninfected) TNF-alpha was added to the HUVEC cultures. The TER was measured at 4, 8, 24, 48 and 72 hr after stimulation. Each point represents the mean value of triplicate. Bars indicate SD

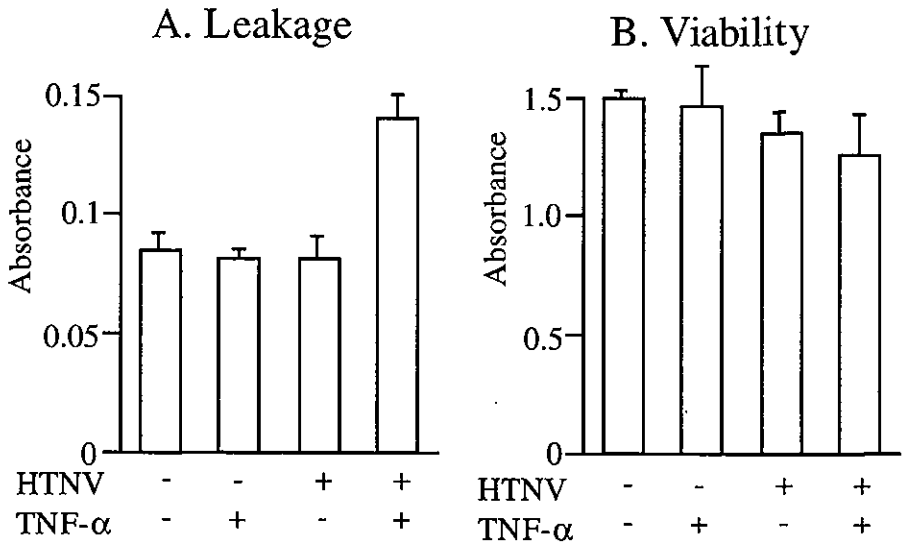

Fig. 2. A. Compatibility of decreased TER with increased permeability. Influx of stained BSA through the HTNV-infected (HTNV+) or uninfected (HTNV−) HUVEC monolayers was quantitated by the absorbance at 48 hr after TNF-alpha stimulation. The TER (average ± SD) at this time point for uninfected unstimulated, uninfected stimulated, infected unstimulated and infected stimulated monolayers were 13.8 ± 0.51, 20.3 ± 0.88, 15.8 ± 0.51 and 8.3 ± 0.33, respectively. **B.** Increased permeability was not due to cell death. Viabilities of HUVEC were examined at 72 hr after TNF-alpha stimulation (1 ng/ml) by the tetrazolim salt color development and shown as the absorbance of each supernatant. Each value represents the mean value of triplicate. Bars indicate SD

and reached the control level within 72 hr. Contrary, the decreased TER did not recover to the untreated level in the HTNV-infected monolayers even at 96 hr. The TER difference between uninfected and HTNV-infected monolayers at 72 hr after stimulation was statistically significant ($p < 0.01$). This decrease of TER was truly induced by TNF-alpha, since the anti-TNF-alpha neutralizing antibody completely abolished the decrease (Fig. 1B). The anti-TNF-alpha antibody itself showed no effect on the TER (data not shown).

To examine if the decreased TER actually reflected the increase in the permeability of monolayers, passive diffusion of BSA through the monolayers was examined (Fig. 2A). At 48 hr, when the HTNV-infected and uninfected monolayers showed significantly different TER ($p < 0.01$), the influx of stained BSA through the infected monolayers was significantly increased ($p < 0.05$) compared to the uninfected ones, indicating that the TER truly reflected the permeability. Further, the increase in permeability was not due to major cell death, since cell viability of these monolayers was not significantly different ($p > 0.05$) between the HTNV-infected and uninfected ones at 72 hr (Fig. 2B).

At any time point of TNF-alpha treatment, the peripheral localization of plakoglobin, which is a sensitive indicator for the matured endothelial cell-to-cell junctions [20], was not disturbed, suggesting that the junction structure was not destroyed by HTNV infection or this TNF-alpha treatment (Fig. 3). These results

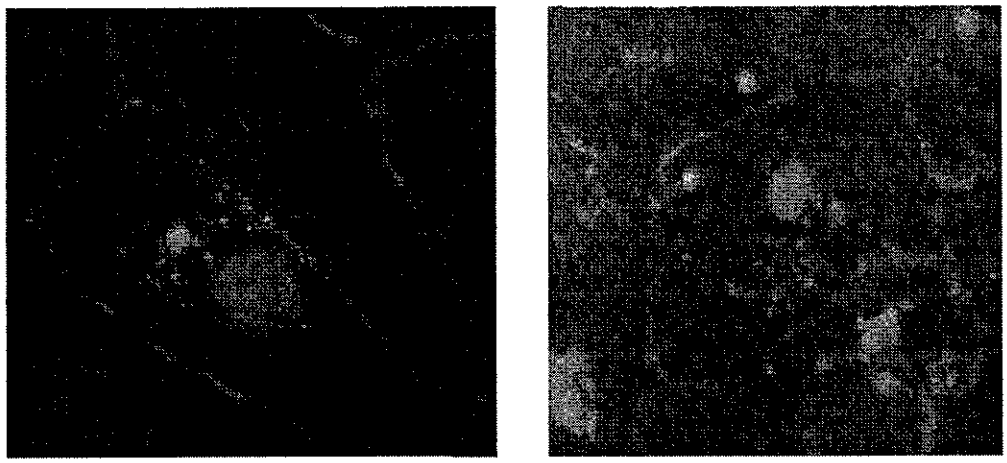

A. Infected B. Uninfected

Fig. 3. Maintenance of cell-to-cell junction structures after TNF-alpha stimulation. HUVEC monolayers were stained by anti-plakoglobin and anti-Seoul virus (cross-reactive with HTNV) antibodies then visualized with FITC (green)- or Rhodamine (red)-labeled secondary antibodies, respectively. **A** HTNV-infected HUVEC at 72 hr after TNF-alpha stimulation. **B** Uninfected non-stimulated control HUVEC at 72 hr

indicate that the HTNV-infected and uninfected HUVEC monolayers show similar levels of initial hyper-permeability without major cell death upon the exposure to TNF-alpha, but the increased permeability remains for a prolonged period in the HTNV-infected monolayers.

Effect of antagonists to NOS and Cox on TNF-alpha-induced hyper permeability

It is known that TNF-alpha induces both nitric oxide (NO) and prostaglandin (PG) through the induction of NOS and Cox-2, respectively. We examined whether NO and PG were involved in the different time courses of the response between HTNV-infected and uninfected monolayers. Aminoguanidine and L-NMA are specific inhibitors for inducible NOS (iNOS) and endothelial NOS (eNOS), respectively. As shown in Fig. 4A and B, neither aminoguanidine (100 μM) nor L-NMA (1 mM) altered the responses of HTNV-infected and uninfected monolayers to 1 ng/ml of TNF-alpha. When 30 μM of indomethacine, a Cox inhibitor was added, TNF-alpha-induced decrease of TER was not affected both in the HTNV-infected and uninfected cell monolayers (Fig. 4C). These results indicate that either NO or PG is not involved in the longer duration of increased permeability in the HTNV-infected monolayers. In fact, neither of them was involved in the TNF-alpha-induced increase in permeability in the HTNV-infected and uninfected monolayers.

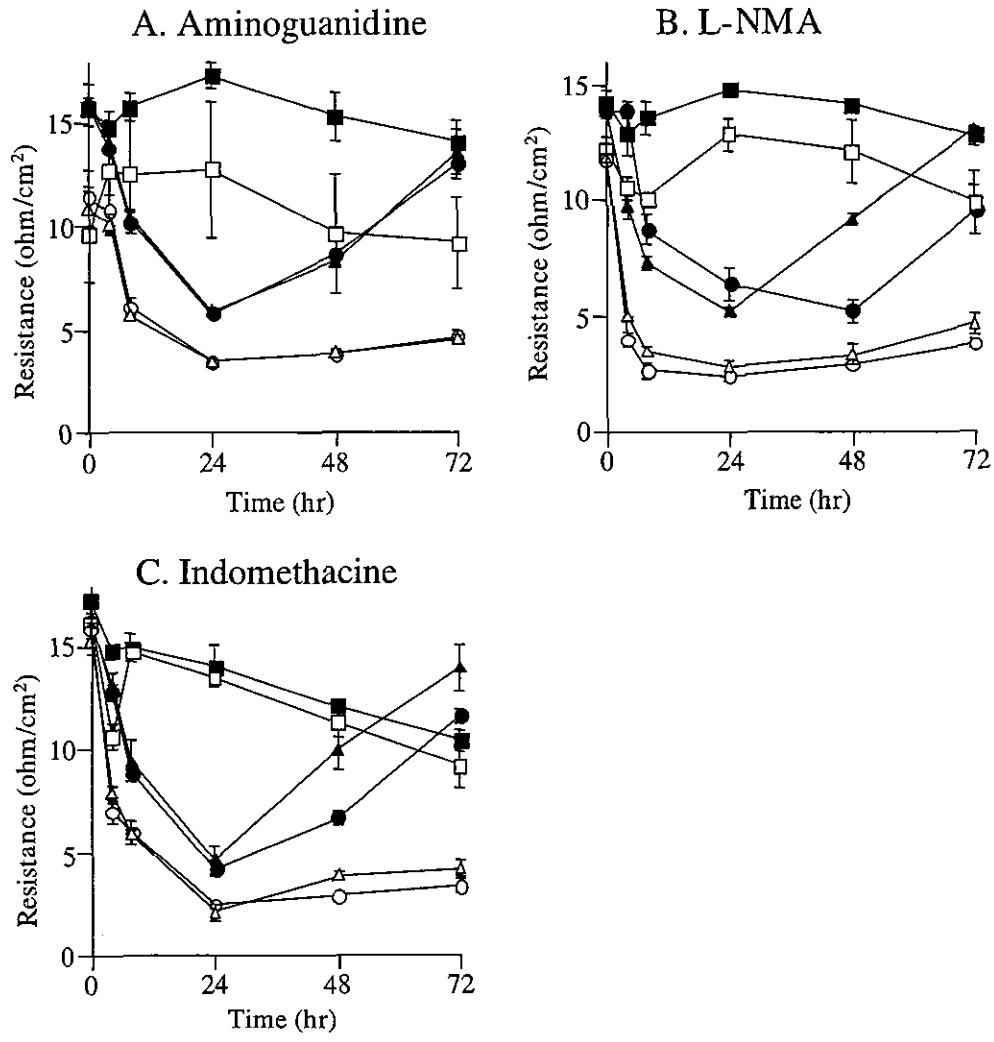

Fig. 4. Absence of the effect of NOS inhibitors and a cyclooxygenase inhibitor on TER. Aminoguanidine (100 μM, iNOS inhibitor, **A**), L-NMA (1 mM, eNOS inhibitor, **B**) or Indomethacin (30 μM, cyclooxygenase inhibitor, **C**) was added along with 1 ng/ml TNF-alpha and the TER was measured at 4, 8, 24, 48 and 72 hr after the stimulation. □, infected control HUVEC; ○, infected TNF-alpha-stimulated HUVEC; △, infected TNF-alpha-stimulated HUVEC with the inhibitor; ■, uninfected control HUVEC; ●, uninfected TNF-alpha-stimulated HUVEC; ▲, uninfected TNF-alpha-stimulated HUVEC with the inhibitor. Each point represents the mean value of triplicate. Bars indicate SD

Induction of pro-inflammatory cytokines by TNF-alpha stimulation

We next asked if the TNF-alpha-induced pro-inflammatory cytokines from endothelial cells might affect the permeability by autocrinal mechanisms. As shown in Fig. 5A, IL-6 was induced at significantly higher levels in the HTNV-infected HUVEC cultures than in the uninfected ones. In the HTNV-infected cells, IL-6 levels increased sharply during the first 24 hr after the stimulation and reached